

## THERMOPHYSICAL PROPERTIES OF MATERIALS

# Application of Two-Parameter Oscillating Interaction Potentials for Specifying the Thermophysical Properties of Simple Liquids

I. K. Loktionov

Donets National Technical University

e-mail: likk@telenet.dn.ua

Received November 24, 2011

**Abstract**—For a statistical description of the equilibrium thermophysical properties of simple liquids, a family of two-parameter oscillating interaction potentials was used. The first-order phase transition was shown to take place in the systems with the model potentials. An analytic relation of the parameters of the potentials with the critical constants was established. The temperature dependences of some thermophysical properties along the line of the phase equilibrium and in the super-critical region  $T > T_c$  were found. The findings were compared to experimental data.

DOI: 10.1134/S0018151X12050094

### INTRODUCTION

The statistical method based on knowledge of the configuration integral (CI) is one of the methods for studying equilibrium thermophysical properties of many-particle systems. Using the CI, one can estimate the phase transition (PT) parameters, phase equilibrium curves, etc., by a given interaction potential.

In [1] the system of  $N$  interacting particles with the pair interaction potential  $v(|\mathbf{r}|)$ , occupying the volume  $V$  at temperature  $T$ , was considered. Provided that the interaction potential can be expanded into the Fourier series by the Gaussian saddle point approximation, the CI expression was obtained in this work. A special case of the nonnegative Fourier transform of a pair potential  $\tilde{v}(k)$  was a matter of issue in [2], where the following expression of the free Helmholtz energy was found:

$$F = -\frac{1}{\beta} \ln Z = F_{\text{id}} - \frac{N}{2} (v(0) - nw) + \frac{V}{2\beta} I(n, \beta). \quad (1)$$

Here,  $F_{\text{id}} = Nk_B T \ln(n\lambda^3)$  is the free energy of an ideal gas;  $n = N/V$  is the particle number density;  $\beta = 1/k_B T$ ;  $k_B$  is the Boltzmann constant;  $\lambda = h/\sqrt{2\pi m_0 k_B T}$  is the thermal de Broglie wavelength;  $h$  is Planck's constant;  $v(0)$  is the potential value for  $r = 0$ ;  $w = \tilde{v}(0)$  is the Fourier transform for  $k = 0$ ;  $m_0$  is the particle mass;  $I(n, \beta) = \int_{\Omega} \frac{d^3k}{(2\pi)^3} \ln(1 + n\beta \tilde{v}(k))$  is the integral determining all the thermodynamic quantities, which depends on both  $n$  and  $\beta$  and the potential parameters;  $\Omega$  is the domain of function  $\tilde{v}(k)$ .

Expression (1) was first obtained in another form in [3] by the collective variables technique. Among the

papers on the topic of the present paper published after [3], of interest are studies [4, 5] where an attempt at systematic presentation of the statistical theory of equilibrium systems was made. The findings were used to specify various systems, e.g., simple liquids, binary alloys, etc. But the oscillating potentials models were not considered in these works at all. In this regard the present paper can bridge this gap. D.N. Zubarev's collective variables technique was developed in recent works particularly on the unified approach to micro-canonical and canonical ensembles of classical statistical mechanics [6, 7].

Based on (1), one can both qualitatively and quantitatively characterize certain thermophysical properties of simple liquids in [2]. In this paper the approximation of free energy (1) is the basis for investigating the PT and thermophysical properties of the systems with pair two-parameter oscillating interaction potentials.

In building up the state equation (SE) of a substance by the statistical physics methods, the problem of choosing an adequate interparticle interaction potential inevitably arises. Since the exact potential form for liquids is unknown, then one has to use the model potentials meeting some general requirements.

The potential should be repulsing at short distances and attracting at long distances, which leads to the appearance of a minimum for the continuous potential functions.

In the context of the theory based on Eq. (1), the investigation is concerned with the systems of particles interacting with a nonnegative Fourier transform through the potential.

The latter requirement arises from approximation (1) employed in this work and ensures the system stability and the existence of the thermodynamic limit [8, 9].

Let us consider the family of the potentials defined by the equations

$$v_m(r) = -\frac{Aa^{2-2m}}{4\pi mr} \sum_{l=1}^m \exp\left(-ar \sin \frac{(2l-1)\pi}{2m}\right) \times \cos\left[\frac{(2l-1)\pi}{m} + ar \cos \frac{(2l-1)\pi}{2m}\right], \quad m = 2, 3, \dots, \quad (2)$$

with the parameters  $A > 0$ ,  $a > 0$ . The cumbersome formula for the potentials (2) is “compensated” by the rather simple single-type form of their Fourier transforms

$$\tilde{v}_m(k) = \frac{A}{k^{2m} + a^{2m}}, \quad (3)$$

which are appealing due to the possibility of analytic representation of the results on thermophysical properties. The potential (2) for  $m = 1$  is a monotonically decreasing function  $r$  which is considered in [2]. For  $m = 2, 3, \dots$ , the trigonometrical functions sine (or cosine) arise in the second member of Eq. (2), so for  $r = 0$  the finite potential function  $v(r)$  becomes oscillating. For example, in the case of  $m = 2$  and  $m = 3$ , the potentials (2) are, respectively,

$$v_2(r) = \frac{A}{4\pi a^2 r} \exp\left(-\frac{ar}{\sqrt{2}}\right) \sin\left(\frac{ar}{\sqrt{2}}\right),$$

$$v_3(r) = \frac{A}{12\pi a^4 r} \times \left[ \exp(-ar) + 2 \exp\left(-\frac{ar}{2}\right) \sin\left(\frac{ar\sqrt{3}}{2} - \frac{\pi}{6}\right) \right].$$

It is easy to verify that with increasing  $m$  the analytic form of potentials becomes much more complicated, so for  $m = 4-6$  we will restrict our consideration to the graphs (Fig. 1) and use the potentials with  $m = 2-6$  for further calculations. There is no strict theoretical justification for the substitution of the “real” potentials like the Lennard–Jones potential with the oscillating potentials of form (2). However, if the influence of the interaction potential’s tail on the substance properties is insignificant [10] and its behavior in the range of short distances qualitatively corresponds to “real” potentials, then the use of oscillating potentials for the calculations of equilibrium thermodynamic properties is expected to give results in agreement with the experimental data. Furthermore, the Fourier transforms (3) make it possible to integrate the SE to completion without any approximation because within the framework of approximation (1) the SE is determined by the Fourier transform of the interaction potential rather than by the potential itself. Thus, the choice was set on the model potentials (2), based on the possibility of solving the posed problem and taking into account their typical behavior.

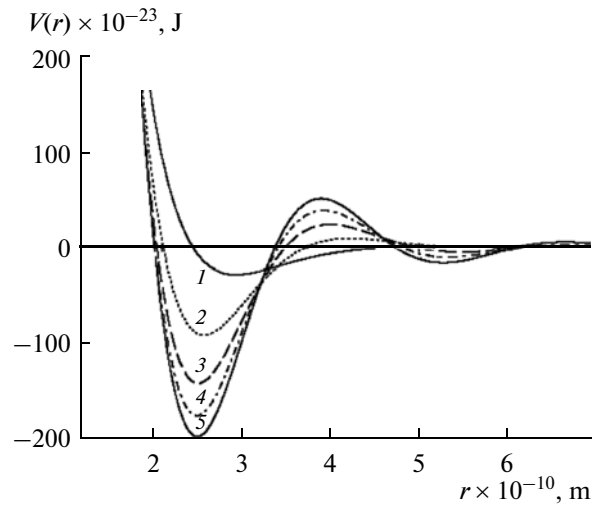


Fig. 1. Potential curves (2). 1,  $m = 2$ ; 2, 3; 3, 4; 4, 5; 5, 6.

## THE STATE EQUATION AND THE CRITICAL POINT PARAMETERS

In order to obtain the SE, we use the known thermodynamic relation connecting pressure with free energy (1)

$$P = -\left(\frac{\partial F}{\partial V}\right)_T = \frac{n}{\beta} + \frac{n^2 w}{2} - \frac{1}{2\beta} \left[ I(n, \beta) - n \frac{\partial I(n, \beta)}{\partial n} \right]. \quad (4)$$

The integral form of the SE (4) is of little use for the applications. So of interest is the problem of integrating  $I(n, \beta)$ , which does not cause any principal difficulties. But before coming to the most essential results, some considerations on calculating  $I(n, \beta)$  must be presented. Let us direct the axis  $z$  along the vector  $k$  and come to spherical coordinates, considering that the Fourier transform is defined by Eq. (3). The angle variable integration results in a one-dimensional integral of the logarithm of the fractional rational function  $k$  over  $k$ . Further integrating by parts, we get

$$I(n, \beta) = \frac{m}{3\pi^2} \left[ b^{2m} \int_0^{+\infty} \frac{k^2 dk}{k^{2m} + b^{2m}} - a^{2m} \int_0^{+\infty} \frac{k^2 dk}{k^{2m} + a^{2m}} \right],$$

$$b^{2m} = a^{2m} + n\beta A,$$

where the extra-integral summands vanish. Application of the residue theory to the obtained integrals results in

$$I(n, \beta) = \frac{a^3 C_m}{6\pi} \left[ (1 + n\beta w)^{\frac{3}{2m}} - 1 \right], \quad C_m = 1 / \sin \frac{3\pi}{2m}. \quad (5)$$

Eq. (5) for  $I(n, \beta)$  can also be obtained without cumbersome calculations using the tabulated values of improper integrals [11].

Values of parameters of oscillating potentials (2)

Potential (2), $m$	$a$ , $10^{10}$ 1/m	$A$ , $10^{21m-50}$ J/m $^{2m-3}$	$Z_c$	$P_c$ , MPa
2	1.8887	2.6236	0.2739	4.6104
3	2.1423	1.6612	0.2749	4.6267
4	2.2352	0.9881	0.2753	4.6335
5	2.2784	0.5716	0.2755	4.6372
6	2.3017	0.3257	0.2756	4.6395

Let us substitute integral (5) into Eq. (4) and get the SE as

$$P = \frac{n}{\beta} + \frac{n^2 w}{2} - \frac{a^3 C_m}{12\pi\beta} \left[ (1+x)^{\frac{3}{2m}-1} \left( 1 - \left( \frac{3}{2m} - 1 \right) x \right) - 1 \right], \quad (6)$$

where  $x = n\beta w$ .

The solution of Eq. (6) together with the set of equations

$$\begin{cases} \left( \frac{\partial P}{\partial n} \right)_c = \frac{1}{\beta_c} \left[ 1 + x_c + \frac{a^3 C_m}{12\pi} \beta_c w \frac{3}{2m} \left( \frac{3}{2m} - 1 \right) \right. \\ \left. \times x_c (1 + x_c)^{\frac{3}{2m}-2} \right] = 0, \\ \left( \frac{\partial^2 P}{\partial n^2} \right)_c = w \left[ 1 + \frac{a^3 C_m}{12\pi} \beta_c w \frac{3}{2m} \left( \frac{3}{2m} - 1 \right) \right. \\ \left. \times (1 + x_c)^{\frac{3}{2m}-3} \left( 1 + \left( \frac{3}{2m} - 1 \right) x_c \right) \right] = 0, \end{cases} \quad (7)$$

containing the nondimensional parameter  $x_c = n_c \beta_c w$ , forms the procedure of determining the critical parameters  $n_c$ ,  $\beta_c$ , and  $P_c$  [12]. The index "c" points to the fact that the values belong to the critical point (CP). Let us express the term  $a^3 C_m \beta_c w / 12\pi$  from the first equation of system (7) and substitute it into the second equation. With a little manipulation, we obtain a linear equation in  $x_c$  and its solution

$$x_c = n_c \beta_c w = \frac{2m}{4m-3}. \quad (8)$$

Substituting  $x_c$  into the first (or the second) equation of system (7), we have

$$\beta_c = \frac{8\pi}{a^3 w C_m} \frac{(4m-3)m}{2m-3} \left( \frac{6m-3}{4m-3} \right)^{\frac{6m-3}{2m}}. \quad (9)$$

Then this is evident from Eq. (8) that the critical particle number equals to

$$n_c = \frac{x_c}{\beta_c w} = \frac{a^3 C_m}{4\pi} \frac{2m-3}{(4m-3)^2} \left( \frac{4m-3}{6m-3} \right)^{\frac{6m-3}{2m}}. \quad (10)$$

Thus, the critical particle number (10) and the temperature (9) in the CP are expressed in terms of the parameters  $A$ ,  $a$  of the interaction potential (2).

To demonstrate the forecasting abilities of approximation (1) together with potentials (2) for  $m = 2-6$  and to calculate their parameters  $A$ ,  $a$ , we will take the

experimental values of argon parameters from the reference-book [13] (density  $\rho_c = 536$  kg/m $^3$ , temperature  $T_c = 150.86$  K, and pressure  $P_c = 5$  MPa) because argon is the most examined and technically significant substance.

The parameter  $a$  is evaluated by substituting  $n_c = \rho_c / m_0$  into (10). To evaluate the parameter  $A$ , we use the equation  $x_c = n_c \beta_c w$  considering  $w = A/a^{2m}$ . Then

$$A = x_c a^{2m} / n_c \beta_c.$$

To estimate the critical pressure, one should substitute the values computed above  $x_c$ ,  $a$ ,  $w$ , and the experimental values  $n_c$  and  $T_c$  into Eq. (6). The values of parameters  $A$ ,  $a$ ,  $Z_c = P_c V / RT_c$ , and  $P_c$ , calculated for  $m = 2-6$ , are given in the table.

Using the data from the table, the oscillating potentials (2) for  $m = 2-6$  are graphed in Fig. 1.

In so far as SE (6) contains only two constants  $A$  and  $a$ , its representation in dimensionless form is possible. Using the reduced variables  $\Pi = P/P_c$ ,  $\varphi = V/V_c$ ,  $\tau = T/T_c$ , SE (6) takes on the form

$$\begin{aligned} \Pi(\varphi, \tau) = \frac{1}{Z_c} \left[ \frac{\tau}{\varphi} + \frac{x_c}{2\varphi^2} - \frac{\tau L_m}{12\pi} \right. \\ \left. \times \left( (q(\varphi, \tau))^{\frac{3}{m}-2} \left( q^2(\varphi, \tau) - \frac{3x_c}{2m\tau\varphi} \right) - 1 \right) \right], \end{aligned} \quad (11)$$

where

$$L_m = 4\pi \frac{(4m-3)^2}{(2m-3)} \left( \frac{6m-3}{4m-3} \right)^{\frac{6m-3}{2m}}, \quad q(\varphi, \tau) = \sqrt{1 + \frac{x_c}{\tau\varphi}}$$

$$Z_c = \frac{P_c V_c}{RT_c} = 1 + \frac{x_c}{2} - \frac{L_m}{12\pi}$$

$$\times \left( (1 + x_c)^{\frac{3}{2m}-1} \left( 1 - \left( \frac{3}{2m} - 1 \right) x_c \right) - 1 \right).$$

This appears to imply that all the model systems the particles of which interact by potentials (2) are thermodynamically similar and follow the law of corresponding states. Thus, for different states with similar  $\tau$ ,  $\varphi$ , and  $\Pi$ , the configurational parts of the given reduced thermodynamic quantities, i.e., entropy, heat capacity, etc., will also coincide.

The behavior of the isotherms graphed in the coordinates of SE (11) is similar to the behavior of the Van

der Waals isotherms, which are known to monotonically decrease with increasing  $\varphi$  for  $\tau \geq 1$  and to have S-shaped loops for  $\tau < 1$ . This indicates the initiation of the first-order PT. At the point with coordinates  $\varphi = 1$ ,  $\Pi = 1$ , which belongs to the critical isotherm  $\tau = 1$ , the isothermal compressibility goes into infinity.

### SATURATION LINE

The phases 1 and 2 of a certain substance can be in equilibrium with each other in the case of the equation of the phase pressures and chemical potentials at temperature  $T < T_c$  ( $\tau < 1$ ). This condition is usually expressed as a set of two equations in two unknowns

$$\begin{cases} \Pi(\varphi_1, \tau) = \Pi(\varphi_2, \tau), \\ \mu(\varphi_1, \tau) = \mu(\varphi_2, \tau), \end{cases} \quad (12)$$

where

$$\begin{aligned} \mu(\varphi, \tau) &= \left( \frac{\partial F}{\partial N} \right)_T \\ &= \frac{\tau}{\beta_c} \left[ \ln \left( \frac{n_c \lambda^3}{\varphi} \right) + \frac{x_c}{\tau \varphi} - \frac{x_c L_m}{8\pi m \tau} \left( 1 - \left( 1 + \frac{x_c}{\tau \varphi} \right)^{\frac{3}{2m-1}} \right) \right] \end{aligned}$$

is the chemical potential.

The equations of set (12) explicitly contain neither critical parameters nor interaction potential parameters. Its solution  $\varphi_1, \varphi_2$  for fixed  $m$  depends on  $\tau$  only, as it is under the law of corresponding states. Nonlinear set (12) allows linearization and representation of  $\varphi_1, \varphi_2$  as the expansion in terms of dimensionless temperature  $\theta = \tau - 1$ . However, the error of the approximate analytical solution increases with moving away from the CP. Therefore, set (12) was solved numerically. The results of solving (12), i.e., the values of reduced phase densities  $\omega_1 = 1/\varphi_1$  and  $\omega_2 = 1/\varphi_2$  at the temperature  $\tau < 1$ , are given in Fig. 2 as the lines of coexisting phases. It is obvious that the measuring data for argon [13] and the results of calculation for all the potentials are rather close for the left branch of curve, which is the vapor condensation curve. For the right branch of the curve, the evaporation curve, the coincidence with the experimental curve is observed at  $0.98 < \tau < 1$ . At temperatures  $\tau < 0.98$ , the quantitative results for the binodal of the liquid phase cannot be admitted to be satisfactory because only the qualitative agreement with the experiment is maintained.

In lowering the temperature, the difference between the theoretical curves and the difference between the theoretical curves and the experimental one increase. The disagreement with the experimental curve diminishes with increasing the number  $m$ . Out of five theoretical curves, curve 6, corresponding to potential (2) for  $m = 6$ , has the minimal error. The performed calculations show the relative error of the pres-

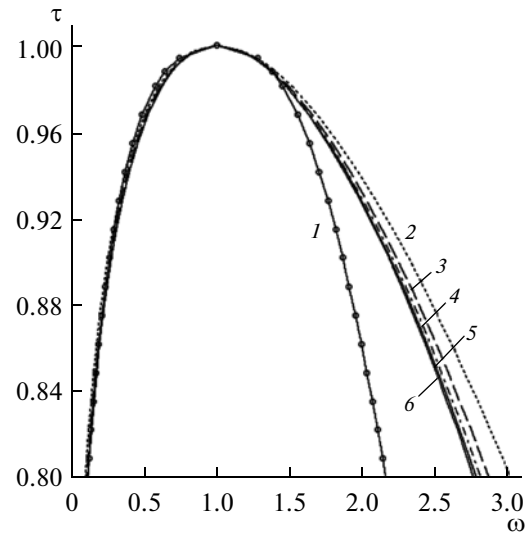


Fig. 2. Lines of coexisting phases. 1, experimental data for argon [13]; 2–6, calculation for  $m = 2-6$  respectively.

sure in the saturation line at temperature  $\tau = 0.8$  to vary between 20% for  $m = 2$  and 6.5% for  $m = 6$ . At temperatures close to the critical one ( $\tau = 1$ ), the relative error for  $m = 2-6$  is equal to 10%. Furthermore, the computed solutions  $\omega_1$  and  $\omega_2$  of set (12) are used for calculating the thermophysical properties in the saturation line.

### THERMODYNAMIC PROPERTIES IN THE SATURATION LINE

Given the free energy  $F$ , it is not difficult to calculate all the molar thermal properties of the system by the thermodynamic identities. To compare the results of calculation, we will use the specific thermal properties from the reference books [13–16]. The relation between the specific value  $X$  and the molar value  $X_M$  is  $X = X_M/M$ . The molar mass of argon is  $M = 0.03994$  kg/mole. The model potentials being two-parameter, all the calculations can be performed in dimensionless units. Let us give the summary of equations to calculate the molar thermodynamic functions, introducing the designation  $q(\omega, \tau) = \sqrt{1 + x_c \omega / \tau}$ .

Entropy

$$\begin{aligned} S &= - \left( \frac{\partial F}{\partial T} \right)_V = R \left[ \frac{5}{2} - \ln \left( \frac{\omega}{\tau^{3/2}} n_c \lambda_c^3 \right) \right. \\ &\quad \left. - \frac{L_m}{12\pi\omega} \left( (q(\omega, \tau))^{\frac{3}{m-2}} \left( q^2(\omega, \tau) - \frac{3}{2m} \frac{x_c \omega}{\tau} \right) - 1 \right) \right], \end{aligned} \quad (13)$$

where  $\lambda_c = h / \sqrt{2\pi m_0 k_B T_c}$ , and  $R = k_B N_A$  is the universal gas constant.

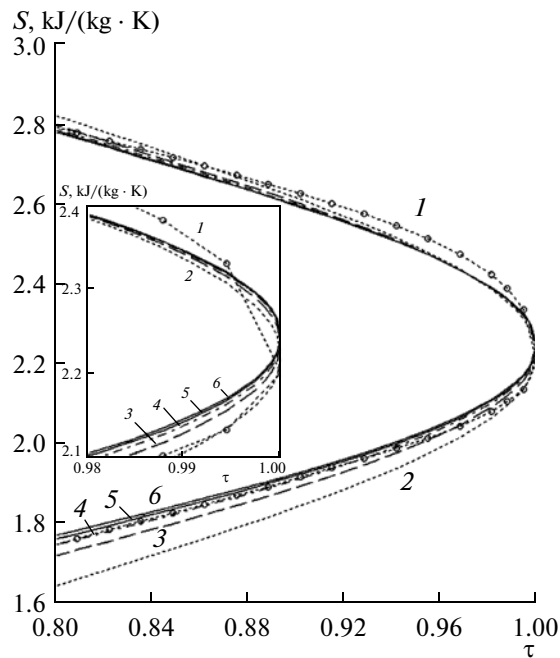


Fig. 3. Dependence of specific entropy on temperature in the saturation line. 1, experiment performed by the data from [13]; curves 2–6, calculation for  $m = 2–6$ .

Isobar thermal capacity

$$C_p = C_v - T \frac{(\partial P / \partial T)_V^2}{(\partial P / \partial V)_T}, \quad (14)$$

where

$$C_v = R \left[ \frac{3}{2} + \frac{L_m}{8\pi m \omega} \left( 1 - \frac{3}{2m} \right) \left( \frac{x_c \omega}{\tau} \right)^2 (q(\omega, \tau))^{\frac{3}{m}-4} \right],$$

$$\left( \frac{\partial P}{\partial T} \right)_V = k_B n_c \left[ \omega - \frac{L_m}{12\pi} \left( q(\omega, \tau) \right)^{\frac{3}{m}-4} \right. \\ \left. \times \left( \left( 1 + \frac{x_c \omega}{\tau} \left( 1 - \frac{3}{2m} \right) \right)^2 + \frac{3}{2m} \frac{x_c \omega}{\tau} \right) - 1 \right],$$

$$\left( \frac{\partial P}{\partial V} \right)_T = - \frac{n_c^2}{\beta_c N_A} \tau \omega^2$$

$$\times \left[ (q(\omega, \tau))^2 - \frac{L_m}{8\pi \omega m} \left( \frac{x_c \omega}{\tau} \right)^2 \left( 1 - \frac{3}{2m} \right) (q(\omega, \tau))^{\frac{3}{m}-4} \right].$$

Enthalpy

$$H = U + PV, \quad (15)$$

where

$$U = F - T \left( \frac{\partial F}{\partial T} \right)_V \\ = R\tau T_c \left[ \frac{3}{2} + \frac{x_c \omega}{2\tau} + \frac{x_c L_m}{8\pi m \tau} \left( (q(\omega, \tau))^{\frac{3}{m}-2} - 1 \right) \right]$$

is the internal energy.

The experimental and theoretical temperature dependences of the specific entropy (13) of argon in

the gaseous (upper branch) and liquid (lower branch) phases in the saturation line are shown in Fig. 3. The upper branches of curves 1–6 are separated from the lower ones by the points of tangency of them and the straight line  $\tau = 1$ .

The results of calculating the specific isobar thermal capacity of the gaseous and liquid argon by Eq. (14) for  $m = 2–6$  and the experimental curve  $C_p(T)$  in the saturation line are shown in Fig. 4.

The experimental dependence and the results of calculating the specific enthalpy of argon in gaseous and liquid states in the saturation line by (15) are given in Fig. 5. The points of contact of the straight line  $\tau = 1$  and curves 1–6 break each of them into two branches. The upper branches of the curves represent the dependence  $H(T)$  for the gaseous state, and the lower ones relate to the liquid state.

### THERMODYNAMIC QUANTITIES IN THE SUPERCRITICAL STATE

In order to get the temperature dependences of the thermodynamic quantities at temperatures  $T > T_c$ , one should find the matter density  $\omega = n/n_c$  in the state characterized by temperature  $\tau$  and pressure  $\Pi$ . Therefore, the problem of calculating the thermophysical properties comes to the solution of a nonlinear equation in the reduced density  $\omega$  at given temperature  $\tau$  and pressure  $\Pi$

$$\Pi(\omega, \tau) - \Pi = 0 \quad (16)$$

In Eq. (16) the reduced SE, obtained from (11) by replacing  $\phi$  with  $1/\omega$ , is denoted by  $\Pi(\omega, \tau)$ . The exact analytical solution of Eq. (16) is very troublesome. In this connection its roots  $\omega$  are evaluated numerically for the values  $\Pi$  and  $\tau$ , corresponding to the measurement parameters  $P$  and  $T$ . One should note that the most extensive data on the thermophysical properties of argon in the supercritical state is presented for pressure  $P = 10$  MPa. Therefore, all the calculations were performed for  $P = 10$  MPa in the temperature intervals taken from reference tables [13–16]. Using Eqs. (13)–(15) and solving Eq. (16) by one of the numerical methods, one can get the temperature dependences of entropy, isobar thermal capacity, and enthalpy. In Figs. 6–8 the results of calculating  $S(T)$ ,  $C_p(T)$ , and  $H(T)$  were correlated with the corresponding experimental curves.

It was found experimentally in [13, 14, 16] that there are the maximums in the curves  $C_p(T)$  in the isobars in the supercritical region, and they decrease with shifting to the right by the temperature axis and increasing pressure. The models considered also predict this effect related to the derivative extremes  $(\partial P / \partial n)_T$ . The maximum in the experimental curve  $C_p(T)$  at  $P = 10$  MPa is reached at  $T = 170$  K according to [13, 14] and at  $T = 172$  K according to [16]. As is obvious from Fig. 7, in the theoretical curves this max-

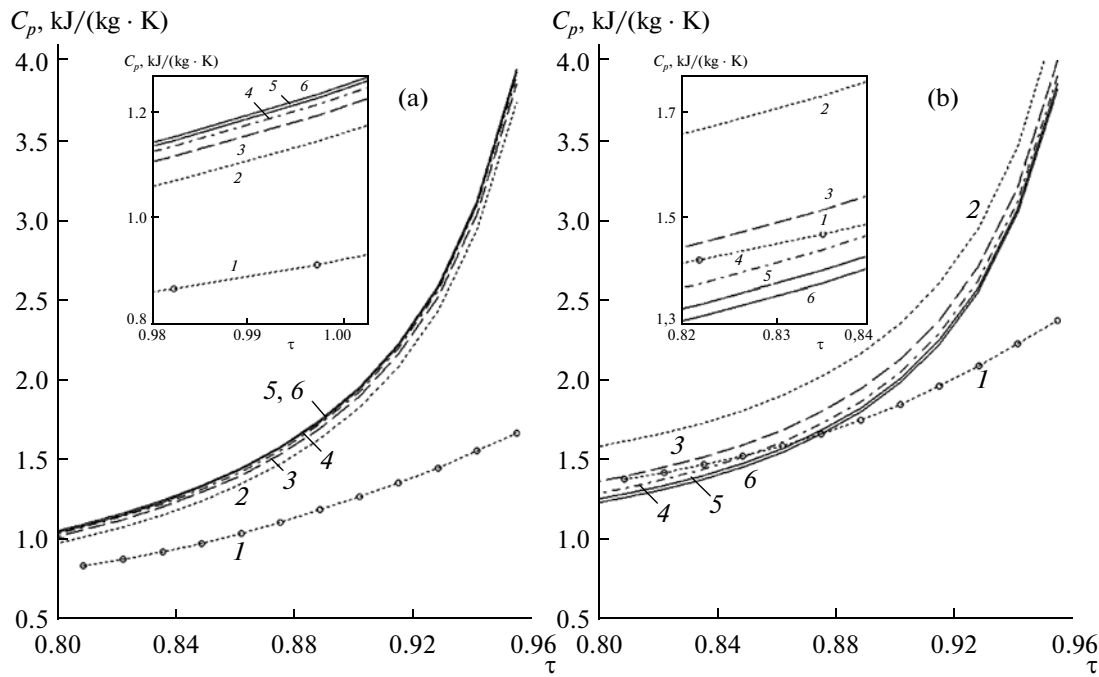


**Fig. 4.** Specific isobar thermal capacity dependence in the saturation line. Gaseous argon (a): 1, experiment performed by the data from [14]; liquid argon (b): 1, experiment performed for the data from [13]; curves 2–6, calculation for  $m = 2-6$ .

imum is slightly higher than the experimental value and it appears at temperatures between 172 and 174 K depending on  $m$ .

It can be noted, that as the temperature rises, the agreement of the theory with the experience improves, and as  $T$  approaches the CP, the agreement decays. This

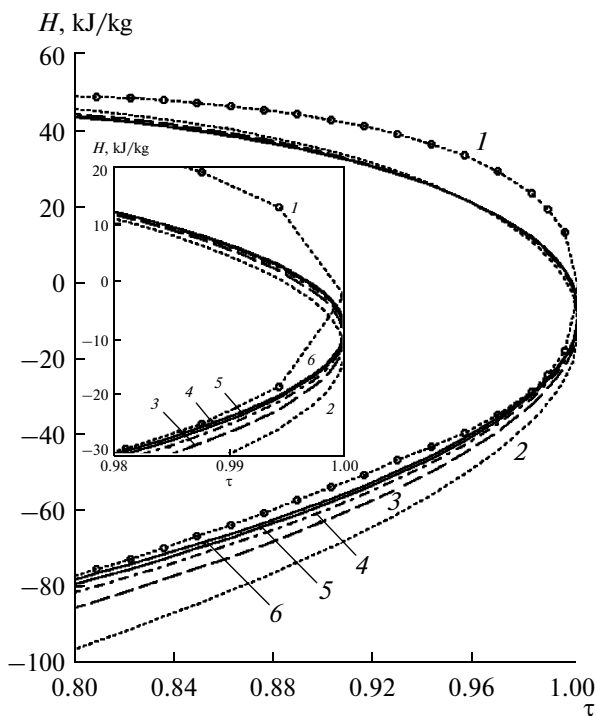


**Fig. 5.** Specific enthalpy dependence in the saturation line. 1, experiment performed by the data from [13]; 2–6 are calculation for  $m = 2-6$ .

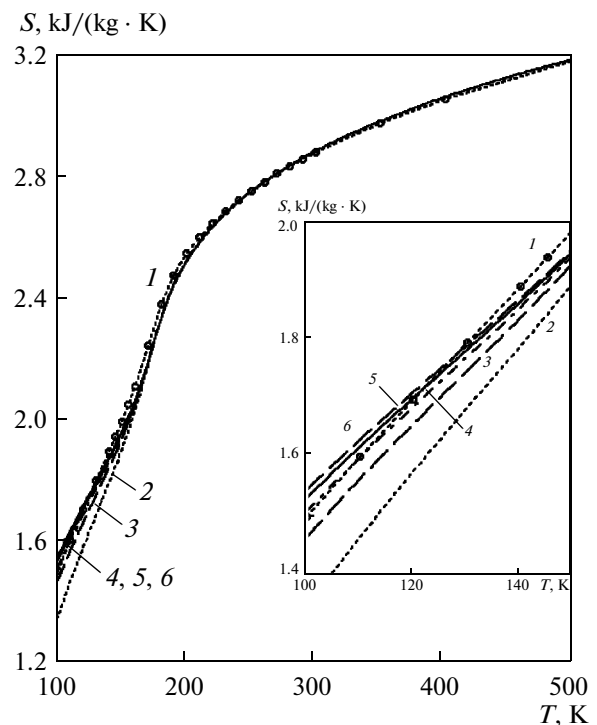


**Fig. 6.** The temperature dependence of the specific entropy of argon vapor at constant pressure. 1, experiment performed by the data from [13]; 2–6 are calculation for  $m = 2-6$ .

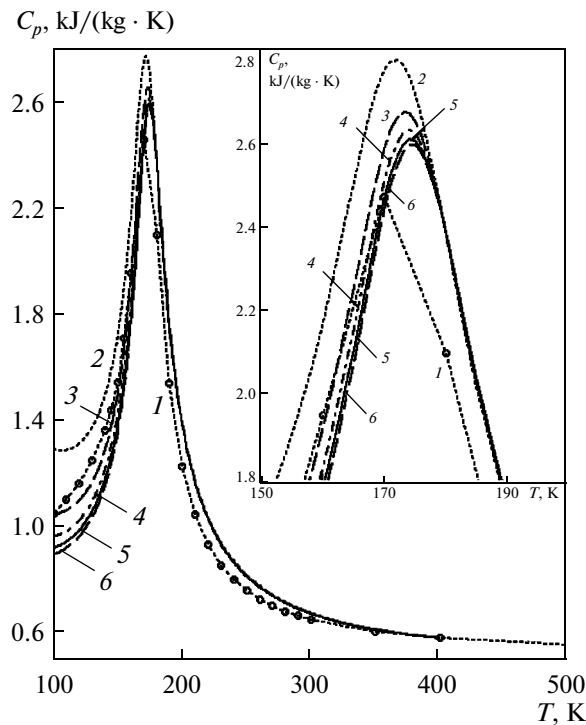


Fig. 7. The temperature dependence of the specific isobar thermal capacity of argon vapor. 1, experiment performed by the data from [13]; 2–6 are calculation for  $m = 2-6$ .

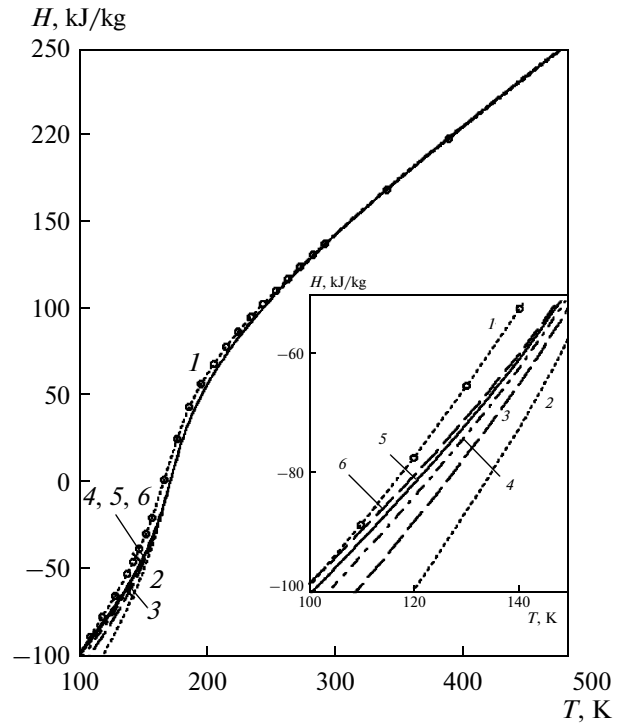


Fig. 8. The temperature dependence of specific enthalpy of argon vapor at constant pressure. 1, experiment performed by the data from [13]; 2–6 are calculation for  $m = 2-6$ .

is clearly demonstrated by the calculations of entropy, thermal capacity, and enthalpy shown in Figs. 6–8. In addition, it is important to emphasize the decrease in the error of calculations with increasing the pressure up to  $\pi \approx 5$ . But SE (11) is found to be ineligible in the region of extremely high pressures, where the contribution of the repulsion branch of the interaction potential seems to be more significant. One of the reasons for the considerable deviation of the calculation results from the experimental data is the insufficiently intensive repulsion of the model potentials as compared to the “real” potentials. Another reason can be related to ignoring the influence of many-particle forces.

Supposing the derivatives  $(\partial P/\partial T)_V$  and  $(\partial P/\partial n)_T$  are found, one can easily calculate the sound velocity and the Joule–Thomson coefficient, which are specified by the relations [17]:

$$u = v \sqrt{\frac{T}{C_V} \left( \frac{\partial P}{\partial T} \right)_V^2 - \left( \frac{\partial P}{\partial v} \right)_T}, \quad (17)$$

$$\alpha = \frac{N_A}{C_P M n} \left[ \frac{T (\partial P/\partial T)_V}{n (\partial P/\partial n)_T} - 1 \right], \quad (18)$$

where  $\left( \frac{\partial P}{\partial v} \right)_T = -\frac{n}{v} \left( \frac{\partial P}{\partial n} \right)_T$  is the derivative with respect to the specific volume  $v = 1/\rho$ ;  $\rho$  is the matter density;

$C_V$ ,  $C_P$  are the specific isochoric and isobar thermal capacities.

In Fig. 9 the experimental and theoretical dependences  $u(T)$  at constant pressure are shown. The data on measuring the sound velocity at  $P = 10$  MPa, reported in [13], are bounded from below with a temperature  $T = 240$  K. Therefore, at  $T < 240$  K the values of  $u$  from [16] are used.

The occurrence of the minimum in the curves  $u(T)$ , as far as the maximum in the lines  $C_p(T)$ , can be connected to the occurrence of the extreme of the pressure derivative with respect to density. In Fig. 9 the minimum in the theoretical curves for  $m = 2-6$  is seen to be reached at temperatures from 172 to 174 K. Two facts attract attention in the given graphs: firstly, the closeness of the theoretical curves at  $T > 150$  K on the selected scale, and secondly, the notable difference between the experimental and theoretical curves. The first fact can mean that the sound velocity is weakly sensitive to the shape of the interaction potential (2); i.e., it depends weakly on  $m$  unlike other thermal characteristics. The second fact is because the isochoric thermal capacity, determined in approximation (1), does not specify the measuring data properly.

It should be noted that the maximums in the curves  $\alpha(T)$  at constant pressure in the above-critical region, similarly to the maximums of  $C_p(T)$ , diminish and shift to the right by the temperature axis with the pres-

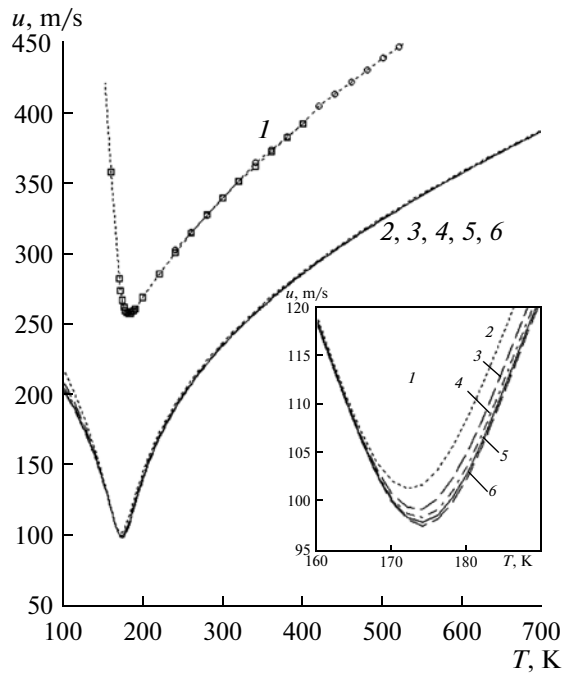


**Fig. 9.** Dependence of sound velocity on the temperature for argon at  $P = 10$  MPa. *I*, experiment performed by the data from [13, 16]; 2–6 are calculation for  $m = 2–6$  by (17).

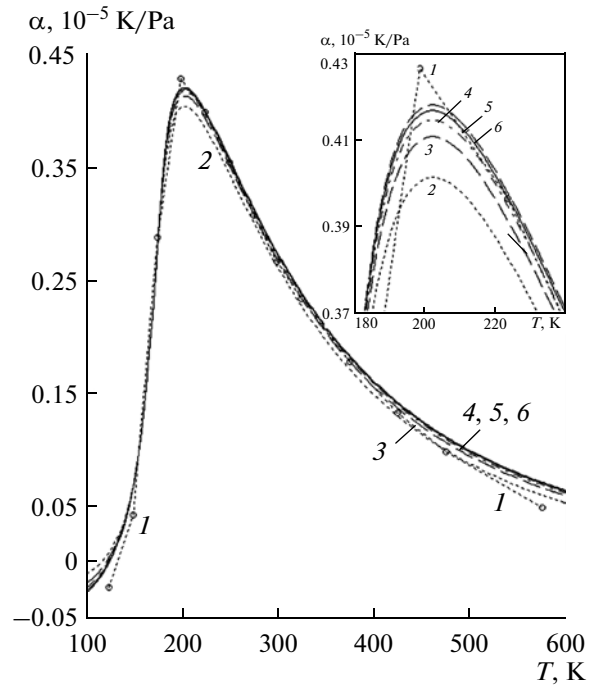


**Fig. 10.** Joule–Thomson coefficient dependence for argon at  $P = 10$  MPa. *I*, experiment performed by the data from [15]; 2–6 are calculation for  $m = 2–6$  by (18).

sure increase [15]. This experimental picture is described within the approach under consideration. The Joule–Thomson coefficient versus temperature curves at  $P = 10$  MPa are given in Fig. 10. The curves 2–6 were plotted for the results of calculation performed by Eq. (18) for  $m = 2–6$ . The closest fit to the measuring data in the vicinity of the maximum is observed for curve 6. The maximum in the experimental curve is reached at  $T = 198$  K, and in the theoretical curves, it is reached at temperatures from 201 to 202 K.

## CONCLUSIONS

Within the framework of the considered approach of oscillating potentials, it has been possible not only to show the qualitative behavior of the single-component systems, but also to investigate their quantitative behavior. The principal findings of our investigation are the following.

—The first-order PT was established to occur in the systems with model potentials.

—An analytical connection between the parameters of potentials and the CP coordinates was obtained.

—In the phase equilibrium line, the theory is shown to give correct qualitative description of thermal properties, but, unfortunately, insufficient accuracy of numerical evaluation of the isobar thermal capacity.

—Calculating the properties at constant pressure in the above-critical region leads generally to satisfactory quantitative results if we compare them to the measuring data.

These circumstances can serve as arguments for the applicability of oscillating potentials within the framework of approximation (1) for specifying the thermal properties of simple liquids, and they suggest that these potentials can be used as a suitable zeroth approximation when considering the thermodynamics of the model systems with multiparameter potentials generated from the “elementary” potentials of form (2) in order to refine the theoretical calculations. When it is considered that the major equilibrium properties of the system, consisting of the particles with short-range interaction, are determined by the potential behavior at short distances, then obtaining rather reasonable results for the oscillation potentials does not seem unexpected [18, 19].

The false prediction of  $C_V(T)$  behavior should be considered as one of the disadvantages of the theory. Hence, the sound velocity dependence  $u(T)$  does not specify quantitatively the actual situation correctly. But these drawbacks seem to be typical for approximation (1) and do not depend on the type of interaction potential if  $\tilde{v}_m(k) > 0$ .

The temperature dependences of the thermal properties obtained in this work do not contain any parameters of potentials, but rather the number  $m$ . The substance identity remains only as the density and tem-



perature in the CP, which enter the design equations. It worth noting that satisfactory results, describing the major experimental data collection, are obtained without any supplementary assumptions. All the qualitative laws demonstrated for the model potentials with  $m = 2-6$  are also true for the model potentials with  $m > 6$ , and a slight improvement of agreement with the experimental results is observed then.

#### ACKNOWLEDGMENTS

The author is grateful to A.Yu. Zakharov for careful reading of the manuscript and helpful discussions.

#### REFERENCES

1. Zakharov, A.Yu. and Loktionov, I.K., *Theor. Math. Phys.*, 1999, vol. 119, no. 1, p. 532.
2. Loktionov, I.K., *High Temp.*, 2011, vol. 49, no. 4, p. 512.
3. Zubarev, D.N., *Dokl. Akad. Nauk SSSR*, 1954, vol. 95, no. 4, p. 757.
4. Yukhnovskii, I.R. and Golovko, M.F., *Statisticheskaya teoriya klassicheskikh ravnovesnykh sistem* (The Statistical Theory of Classical Equilibrium Systems), Kiev: Naukova Dumka, 1980, p. 372.
5. Yukhnovskii, I.R., *The Theory of Phase Transitions of the Second Order: Collective Variables Method*, Singapore: World Scientific, 1987.
6. Zakharov, A.Yu., *Russ. J. Phys. Chem. A*, 2000, vol. 74, no. 1, p. 40.
7. Zakharov, A.Yu., *Izv. Akad. Nauk, Ser. Fiz.*, 2004, vol. 68, no. 7, p. 938.
8. Baus, M. and Tejero, C.F., *Equilibrium Statistical Physics: Phases of Matter and Phase Transitions*, Brussels: Springer, 2008.
9. Ruelle, D., *Statistical Mechanics: Rigorous Results*, New York: Benjamin, 1969.
10. Verlet, L., *Phys. Rev.*, 1968, vol. 165, no. 1, p. 201.
11. Prudnikov, A.P., Brychkov, Yu.A., and Marichev, O.A., *Integrals and Series*, New York: Gordon and Breach, 1986.
12. Loktionov, I.K., *High Temp.*, 2012, vol. 50, no. 3, p. 359.
13. Vargaftik, N.B., *Tables on the Thermophysical Properties of Liquids and Gases*, New York: Wiley, 1975.
14. Rabinovich, V.A., Vasserman, A.A., Nedostup, V.I., and Veksler, L.S., *Thermophysical Properties of Neon, Argon, Krypton, and Xenon*, Bristol: Hemisphere, 1988.
15. *Tablitsy fizicheskikh velichin. Spravochnik* (Tables of Physical Quantities: A Reference Book), Kikoin, I.K., Ed., Moscow: Atomizdat, 1976.
16. Younglove, B.A., *J. Phys. Chem. Ref. Data*, 1982, vol. 11, no. Suppl. 1, p. 353.
17. Sychev, V.V., *The Differential Equations of Thermodynamics*, New York: Taylor and Francis, 1991.
18. Bushman, A.V. and Fortov, V.E., *Phys.—Usp.*, 1983, vol. 26, no. 6, p. 465.
19. Martynov, G.A., *Phys.—Usp.*, 1999, vol. 42, no. 6, p. 517.